A core catalytic domain of the TyrA protein family: arogenate dehydrogenase from *Synechocystis*

Carol A. BONNER*, Roy A. JENSEN*†‡, John E. GANDER* and Nemat O. KEYHANI*[1]

*Department of Microbiology and Cell Science, Bldg 981, PO Box 110700, University of Florida, Gainesville, FL 32611, U.S.A., †Biosciences Division, Los Alamos National Laboratory, Los Alamos, NM 87544, U.S.A., and ‡Department of Chemistry, City College of New York, New York, NY 10031, U.S.A.

The TyrA protein family includes prephenate dehydrogenases, cyclohexadienyl dehydrogenases and $TyrA_a$s (arogenate dehydrogenases). *$tyrA_a$* from *Synechocystis* sp. PCC 6803, encoding a 30 kDa $TyrA_a$ protein, was cloned into an overexpression vector in *Escherichia coli*. $TyrA_a$ was then purified to apparent homogeneity and characterized. This protein is a model structure for a catalytic core domain in the TyrA superfamily, uncomplicated by allosteric or fused domains. Competitive inhibitors acting at the catalytic core of TyrA proteins are analogues of any accepted cyclohexadienyl substrate. The homodimeric enzyme was specific for L-arogenate ($K_m = 331\ \mu M$) and $NADP^+$ ($K_m = 38\ \mu M$), being unable to substitute prephenate or NAD^+ respectively. L-Tyrosine was a potent inhibitor of the enzyme ($K_i = 70\ \mu M$). NADPH had no detectable ability to inhibit the reaction. Although the mechanism is probably steady-state random order, properties of 2′,5′-ADP as an inhibitor suggest a high preference for L-arogenate binding first. Comparative enzymology established that both of the arogenate-pathway enzymes, prephenate aminotransferase and $TyrA_a$, were present in many diverse cyanobacteria and in a variety of eukaryotic red and green algae.

Key words: arogenate dehydrogenase, enzyme specificity, prephenate, *Synechocystis*, TyrA, tyrosine.

INTRODUCTION

Dehydrogenases dedicated to TYR (L-tyrosine) biosynthesis comprise the TyrA protein family, an assemblage of homologues having different substrate specificities. A given TyrA protein may be specific for AGN (L-arogenate) for prephenate or may be able to accept either of these cyclohexadienyl substrates. This dehydrogenase protein family also exhibits comparable diversity with respect to its nicotinamide nucleotide co-substrate. Thus a given TyrA enzyme having any of the aforementioned specificities for cyclohexadienyl substrate may be specific for NAD^+, for $NADP^+$ or may utilize either. This harmonizes with recent reports [1,2] that substrate specificity often varies across a given protein family, even though the basic reaction chemistry deployed is usually maintained throughout the family. In instances of broad substrate specificity, there is variation in that alternative substrates may in some cases be accepted equally well, but in other cases one substrate may be preferred by an order of magnitude or more. Table 1 provides a key to the nomenclature used to describe the various possible cyclohexadienyl substrate combinations exhibited by TyrA proteins.

$TyrA_a$ (arogenate dehydrogenase) was first discovered in several species of cyanobacteria [3]. Until that time the only known route to TYR biosynthesis was via the coupled activities of prephenate dehydrogenase and aromatic aminotransferase. Although prephenate dehydrogenase activity was not detected in the cyanobacterium studied by Stenmark et al. [3], prephenate was consumed in the presence of an amino acid. This suggested that transamination at the side-chain position might precede the oxidative decarboxylation event that yields the aromatic ring of TYR. Both the transaminase (prephenate aminotransferase) and the dehydrogenase ($TyrA_a$) were partially purified, and the new intermediate compound was named pretyrosine. Since pretyrosine was later shown in some organisms to also act as a precursor of PHE (L-phenylalanine) [4], it was renamed L-arogenate (meaning ‘giving rise to aromatics’) [5]. A composite diagram of the dual biochemical flow routes to TYR is shown in Figure 1. This series of reactions is preceded upstream by the catalytic condensation of erythrose 4-phosphate and phosphoenolpyruvate by 3-deoxy-D-*arabino*-heptulosonate 7-phosphate synthase, followed by six enzymic steps to form chorismate, the central branch-point intermediate of the pathway. L-Tryptophan is formed from chorismate in five overall reaction steps (results not shown), involving seven catalytic domains (see [6] and references therein). Prephenate, formed from chorismate by the action of chorismate mutase, is the common precursor that feeds into the two divergent pathways that ultimately yield PHE (results not shown) and TYR.

Since the discovery of AGN, combinatorial variations of the dual pathways leading to PHE and TYR synthesis have been documented. For instance, *Brevibacterium flavum* utilizes AGN as the sole precursor of TYR [7,8], but uses phenylpyruvate as the sole precursor of PHE [9]. In opposite symmetry, *Pseudomonas diminuta* uses AGN to form PHE, but uses 4-hydroxyphenylpyruvate as the precursor of TYR [10]. *Ps. aeruginosa* deploys both of the foregoing routes to PHE and to TYR [4]. A single broad-specificity cyclohexadienyl dehydrogenase ($TyrA_c$) accounts for the ability of *Ps. aeruginosa* to use prephenate or AGN as alternative substrates for TYR biosynthesis [11]. On the other hand, the presence of two distinct and spatially separated enzyme systems accounts for the *Ps. aeruginosa* pathway duality to PHE, i.e. (i) a bifunctional cytoplasmic protein AroQ•PheA that contains fused catalytic domains for chorismate mutase (AroQ) and prephenate

Abbreviations used: AGN, L-arogenate; DTT, dithiothreitol; LB, Luria–Bertani; PHE, L-phenylalanine; TYR, L-tyrosine; $TyrA_a$, arogenate dehydrogenase; for brevity, single-letter code has been used for amino acids; for example, H197 stands for His-197.

[1] To whom correspondence should be addressed (email keyhani@ufl.edu).

The nucleotide and the deduced amino acid sequences corresponding to the *Synechocystis* sp. PCC 6803 cloned *$tyrA_a$* gene reported in this paper have been submitted to the DDBJ, EMBL, GenBank® and GSDB Nucleotide Sequence Databases under the accession number AF482689.

Table 1 Nomenclature used to distinguish substrate specificities

Abbreviation*		
Gene	Gene product	Description of specificity†
tyrA$_x$	TyrA$_x$	Specificity for cyclohexadienyl substrate is unknown
tyrA$_c$	TyrA$_c$	Cyclohexadienyl dehydrogenase (CDH)
tyrA$_p$	TyrA$_p$	Prephenate dehydrogenase (PDH)
tyrA$_{(p)}$	TyrA$_{(p)}$	Cyclohexadienyl dehydrogenase utilizes prephenate at least 10-fold better than L-arogenate
tyrA$_a$	TyrA$_a$	Arogenate dehydrogenase (ADH)

* Abbreviation subscripts indicate the specificities for the cyclohexadienyl substrate.

† The abbreviations CDH, PDH and ADH (shown parenthetically) have been used frequently in the literature.

dehydratase (PheA) [12] and (ii) a periplasmic cyclohexadienyl dehydratase (PheC) [13]. PheC has dual-substrate specificity and can either convert prephenate into phenylpyruvate or AGN into PHE. The 'prephenate dehydrogenase' of enteric bacteria is technically a cyclohexadienyl dehydrogenase, since it has a documented capability to utilize AGN, although activity with prephenate is superior by an order of magnitude [14]. We denote such cyclohexadienyl dehydrogenases as TyrA$_{(p)}$ (Table 1). In plants, the AGN route seems to be the major, if not the only, pathway leading to both PHE and TYR syntheses [15–17].

Cyanobacteria comprise a cohesive but internally diverse lineage and, since the earliest studies [3], it has eventually become apparent that various species exhibit individuality in the profile of substrates utilized by their TyrA enzymes [18]. Genomic results are now revealing the extent to which this can be attributed to the presence of a single broad-specificity TyrA$_c$ on the one hand, or to multiple *tyrA* genes encoding enzymes of different substrate specificity on the other. TyrA$_a$ from the original cyanobacterial strain that was studied most, *Agmenellum quadruplicatum* BG1 (renamed *Synechococcus* sp. ATCC 29404), differs from the TyrA$_a$ of *Synechocystis* sp. PCC 6803 studied here, in being insensitive to TYR inhibition and in being able to use NAD^+ almost as well as $NADP^+$ [3]. Previously, cloned microbial TYR-pathway dehydrogenases have been limited to those specific for

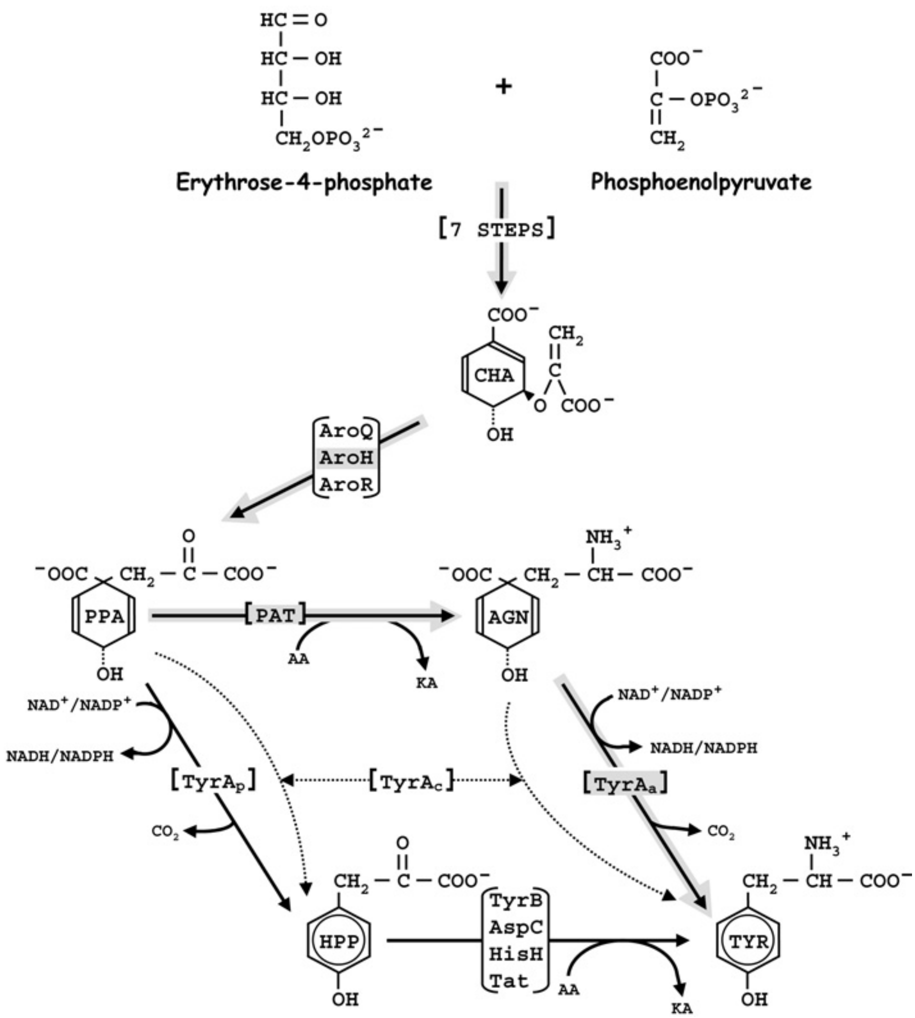

Figure 1 Composite of alternative biochemical routes to TYR in nature

Chorismate (CHA) is converted into prephenate (PPA) via chorismate mutase, which is represented in Nature by three homology groups (AroQ, AroH or AroR) [12]. PPA may be transaminated by prephenate aminotransferase (PAT) to yield AGN. TyrA$_a$ converts AGN into TYR. Alternatively, TyrA$_p$ converts PPA into 4-hydroxyphenylpyruvate (HPP) that is then transaminated to TYR via (depending on the organism) a homologue of either TyrB, AspC, HisH or Tat [58]. A broad-specificity cyclohexadienyl dehydrogenase (TyrA$_c$) is competent to catalyse either the TyrA$_a$ or the TyrA$_p$ reaction (shown by dotted arrows). The *Synechocystis* sp. enzyme route to TYR is highlighted in grey. Other abbreviations: AA, amino-acid donor; KA, oxo-acid accepter.

prephenate, or those with broad-substrate specificity, all examples so far being about those that utilize NAD^+ as the cofactor (see [19] and references therein). In the present study, we demonstrate that the single gene present in *Synechocystis* PCC 6803 encodes a TyrA protein that is absolutely specific for both AGN and $NADP^+$. TYR, the sole inhibitor molecule recognized, is quite effective.

TyrA proteins vary from those that possess only a basic catalytic core compared with others that possess allosteric domains and/or fusion domains [19]. The fusion of the enteric *tyr*$A_{(p)}$ gene with *aro*Q (encoding chorismate mutase) promotes an interesting additional specificity determinant in that the dehydrogenase domain will be preferentially exposed to prephenate in its catalytic microenvironment due to the proximity of the fused AroQ domain (which generates prephenate). Analysis of $TyrA_a$ in *Synechocystis*, which possesses only the basic catalytic module, allows the study of properties of this core domain, uncomplicated by any effect of allosteric or other domains.

MATERIALS AND METHODS

Materials

Buffers, reagents and cell culture media were purchased from commercial sources. AGN and barium prephenate (converted into the potassium salt before the enzyme assay) were > 90 % pure and prepared as described in [20]. Reagents for molecular biology were obtained from New England Biolabs (Beverly, MA, U.S.A.), Stratagene (La Jolla, CA, U.S.A.) and Promega (Madison, WI, U.S.A.). *Escherichia coli* strain BL21(DE3) (Novagen; Madison, WI, U.S.A.), harbouring designated plasmid constructs where indicated, were stored as frozen cultures in LB (Luria–Bertani) broth supplemented with 10 % (v/v) glycerol. Molecular-mass standards for gel filtration were purchased from Sigma–Aldrich (St. Louis, MO, U.S.A.). Frozen cell pellets of *Synechocystis* sp. (PCC 6902), *Fisherella* sp. (ATCC 29539), *Anabaena* sp. (PCC 7119), *Synechococcus* sp. (PCC 6301), *Porphyridium cruentum* and *Prochlorothrix hollandica* were generously provided by Geraldine Hall (Elmira College, Elmira, NY, U.S.A.). The cosmid containing the genomic clone CS01241 was kindly provided by CyanoBase (Genome Database for *Synechocystis* sp. PCC 6803, Kazusa DNA Research Institute, Chiba, Japan).

Construction of pET:*tyrA*$_a$, a $TyrA_a$ overexpression vector

DNA preparations, restriction enzyme digests, ligations and transformations were performed using standard techniques. The cosmid clone CS01241, which spans the *Synechocystis* genome between 1 532 800 and 1 570 740 bp, was transformed and maintained in Epicurian Coli™ strain XL1-Blue MR (CyanoBase) [21]. The *tyrA*$_a$ gene was amplified by PCR using appropriate primers. The 5′-PCR primer was designed to include an *Nde*I restriction site (in boldface type below) to facilitate cloning into the ATG start site of pET24b(+) (Novagen), just downstream of the T7 promoter in the overexpression vector. To facilitate directional cloning of the *tyrA*$_a$ gene, an *Xho*I restriction site (underlined) was designed into the 3′-PCR primer. The primers used to construct the overexpression vector were 5′-GATAAA**CATATG**AAAATTGGTGTTGTTGGT-3′ and 5′-GATAAA<u>CTCGAG</u>TTATTCAACATACTTGTCCCGATC-3′. The amplified PCR product (861 kb) was doubly digested with *Nde*I and *Xho*I, ligated directly into an equivalently digested sample of the pET24b(+) vector and transformed into the T7 polymerase-inducible host strain BL21(DE3). The isolated clone in pET24b(+) was confirmed by sequencing the entire insert. Nucleotide and deduced amino acid sequence analyses were performed using web-based software tools.

$TyrA_a$ assays

Three assay methods were used. Two methods involved measurement of the rate of NADPH (or NADH) formation in continuous assays using either fluorimetric or spectroscopic detection systems. Continuous spectroscopic measurements were performed at 340 nm using a Beckman spectrophotometer. Continuous fluorimetric detection of NADPH at an excitation wavelength of 340 nm and an emission wavelength of 460 nm was performed with a Shimadzu spectrophotofluorimeter. Based on standard-curve values of authentic NADPH, a conversion factor of 23 FU (fluorescent units) = 1 nmol/min NADPH was used in calculations of enzyme activity. The highly sensitive fluorimetric assay was used for kinetic studies of purified protein to ensure that initial rates as accurate as possible could be obtained at low substrate concentrations. For kinetic studies, initial rates were measured using the combinations of substrate specified in Figures 4 and 5. The assays for each set of concentrations were performed in triplicate. Initial velocities were determined from the slopes of the progress curve within 90 s of elapsed reaction time, and linear portions of progress curves were used to determine reaction rates. Each data point is the average of three determinations; S.E.M. 2.6 % ($n = 71$).

The third method utilized HPLC (Beckman, Schaumburg, IL, U.S.A.) for direct measurement of TYR formation. A standard reaction mix consisted of 50 mM Epps [4-(2-hydroxyethyl)piperazine-1-propanesulphonic acid] buffer (pH 8.6), 0.5 mM $NADP^+$, 0.08 mM AGN and enzyme at room temperature (25 °C), unless otherwise stated in the text. TYR production was directly confirmed by HPLC assay after the reactions were stopped by the addition of NaOH; the samples were derivatized with *o*-phthalaldehyde for fluorimetric detection of peak area, and then injected into a C-18 reverse-phase column (Altech) as described in [22]. HPLC peak areas of authentic TYR were used to construct a standard curve.

Aminotransferase assay

Aminotransferases were assayed by *o*-phthalaldehyde derivatization of amino acids and fluorimetric detection by HPLC [23]. The substrates for prephenate aminotransferase, prephenate and L-glutamate were transaminated to AGN and α-oxoglutarate respectively. Since L-glutamate and AGN overlap on the HPLC elution profile, samples were acidified, resulting in the quantitative conversion of AGN to PHE. PHE can be readily quantified, since it is eluted well away from both L-glutamate and AGN. For the assay of aromatic aminotransferase, the phenylpyruvate/L-glutamate co-substrates were transaminated to PHE and α-ketoglutarate. When crude extracts were assayed for prephenate aminotransferase, they were incubated for 15 min at 65 °C to inactivate prephenate dehydratase. Prephenate aminotransferase is stable to this heat treatment as commonly found [23], and this procedure is generally successful in avoiding interference of prephenate dehydratase with the assays. Aminotransferase assays consisted of 50 mM Epps buffer (pH 8.6), 5 mM amino acid donor, from 1 to 5 mM oxo-acid acceptor, 0.1 mM pyridoxal 5′-phosphate and enzyme.

Determination of protein concentrations

Protein concentrations were estimated by the Bradford Bio-Rad protein assay [24], using BSA as a standard.

Overexpression and purification of $TyrA_a$

Step 1: crude extracts

A single colony of *E. coli* BL21(DE3) harbouring pET:*tyrA*$_a$ was inoculated into 10 ml of LB medium, supplemented with 30 μg/ml kanamycin and grown overnight at 32 °C with aeration. A 200-ml volume of LB growth medium containing kanamycin was inoculated with 10 ml of the overnight culture. After growth at 32 °C to an absorbance A_{600} 0.5, 1 mM isopropyl β-D-thiogalactoside was added, and the cells were incubated further for 2 h before harvest by centrifugation at 6000 ***g*** for 10 min at 4 °C. The resultant cell pellet (wet weight = 3.44 g) was resuspended in 50 mM Epps buffer (pH 8.6), containing 20 % glycerol and 1 mM DTT (dithiothreitol). The cells were disrupted by sonication (Ultratip Labsonic System), using 3 × 30-s pulses with 2 min of inter-pulse cooling, and cell debris was removed by ultracentrifugation (150 000 ***g***, 1 h at 4 °C). The high-speed supernatant (18 ml) was desalted by passing through a DG30 column (Bio-Rad) equilibrated with 50 mM Epps buffer (pH 8.6), containing 20 % glycerol. The final total volume of the desalted crude extract of 24 ml was used for assay and for purification with an FPLC system (Amersham Biosciences).

Step 2: preparative FPLC anion-exchange (Mono-Q) chromatography

Crude extract from step 1 (2 × 10-ml aliquots) was injected into an ice-jacketed Mono-Q HR 10/10 column (bed volume, 8 ml; Amersham Biosciences), equilibrated in 50 mM potassium phosphate buffer (pH 7.5), containing 20 % glycerol. The column was washed with 3 column volumes of the same buffer, and a gradient (220 ml) from 0 to 0.5 M KCl in the same buffer was applied to the column. Fractions containing activity eluted at approx. 0.2 M KCl, and these were pooled (44.5 ml) and dialysed against 50 mM Epps buffer (pH 8.6), containing 20 % glycerol. A final volume of 45 ml was obtained.

Step 3: 2′,5′-ADP−Sepharose 4B affinity chromatography

Aliquots (1 ml) of the pooled dialysed sample from step 2 were injected on to an ice-jacketed 2′,5′-ADP−Sepharose 4B HR10/10 FPLC column (bed volume, 8.25 ml; Amersham Biosciences), equilibrated in 50 mM Epps buffer (pH 8.6), containing 20 % glycerol. The column was washed with 2 column volumes of the same buffer, and a simultaneous gradient from 0 to 0.4 M KCl and 0 to 0.30 mM $NADP^+$ in the same buffer was applied to the column. Appropriate fractions were pooled, and purity was estimated by SDS/PAGE.

Molecular-mass determination by MS

A sample of pure enzyme was subjected to MALDI−TOF (matrix-assisted laser-desorption ionization−time-of-flight) analysis (Voyager-DE PRO, Applied Biosystems) at the Protein Chemistry Core Laboratory, University of Florida.

Native molecular-mass estimation by size-exclusion chromatography

An FPLC Superdex 75 HR10/30 column (Amersham Biosciences) was used to estimate the native molecular mass of $TyrA_a$. The column was equilibrated in 50 mM Epps buffer (pH 8.6), containing 20 % glycerol and 0.15 M KCl. Purified protein was applied on to the column (200 μl aliquots) and eluted with the same buffer using a flow rate of 0.5 ml/min. Protein standards, including Blue Dextran (2000 kDa), albumin (66 kDa), carbonic anhydrase (29 kDa) and cytochrome *c* (12.4 kDa) were prepared in the same buffer and were applied individually to the column.

SDS/PAGE and N-terminal amino acid determination

Protein samples were denatured by SDS and subjected to SDS/PAGE to estimate monomeric mass following the method of Laemmli [25]. Purified $TyrA_a$ protein was electroblotted from SDS/PAGE to a PVDF membrane (Fisher Scientific, Fair Lawn, NJ, U.S.A.). After transfer, the blot was lightly stained with Coomassie Blue. The N-terminal amino acid sequence of the protein was determined at the Protein Chemistry Core Facilities (University of Florida Biotechnology CORE Center).

Preparation of crude extracts from photosynthetic bacteria and algae

Frozen cell pellets from species of *Synechocystis*, *Synechococcus*, *Fisherella*, *Anabaena*, *P. cruentum*, *P. hollandica* and *Chlorella sorokiniana* were dissolved in 50 mM potassium phosphate buffer (pH 7.5), containing 20 % glycerol, 1 mM pyridoxal 5′-phosphate, 1 mM DTT and 1 mM PMSF. Samples were sonicated, and cell debris was removed by ultracentrifugation at 150 000 ***g*** for 1 h at 4 °C. The resulting supernatant was dialysed against 50 mM potassium phosphate buffer (pH 7.5), containing 20 % glycerol and 1 mM pyridoxal 5′-phosphate, and used as crude extract for enzyme activity assays.

RESULTS

Molecular cloning of *tyrA*$_a$

Homology searching led to the identification of a single *tyrA* gene from *Synechocystis* sp. PCC 6803 (incorrectly annotated as a prephenate dehydrogenase). The nucleotide sequence of *tyrA* displayed a 48.6 % GC content, consistent with the 48.7 % GC genomic average for *Synechocystis* sp. (www.kazusa.or.jp/codon/). The open reading frame corresponding to *tyrA*$_a$ encodes a 279-residue protein with the following predicted parameters: molecular mass of 30.21595 kDa, pI of 5.51 and a molar absorption coefficient ε_{280} of 26 330 $M^{-1} \cdot cm^{-1}$. No signal peptide was found. Primers were designed for cloning *tyrA*$_a$ into the pET24b(+) overexpression vector. Cosmid clone CS01241, containing a 37.9 kb insert of the *Synechocystis* genome, was used as template for amplification of *tyrA*$_a$ in PCR mixtures as described in the Materials and methods section. The resulting construct, designated as pET:*tyrA*$_a$, was used for further characterization. The presence of the pET:*tyrA*$_a$ insert was confirmed by nucleotide sequencing. The nucleotide sequence upstream of the start site contains two closely spaced stop codons and is generally A/T-rich; however, an obvious ribosome-binding site with the conventional spacing was not apparent. The nucleotide and deduced amino acid sequence corresponding to the *Synechocystis* sp. PCC 6803 cloned *tyrA*$_a$ gene has been deposited in GenBank® database and given the accession number AF482689.

Purification and properties of the recombinant $TyrA_a$

The enzyme was purified from recombinant *E. coli* BL21(DE3) cells harbouring pET:*tyrA*$_a$ as described in the Materials and methods section, yielding an apparently homogeneous protein (Figure 2). Little or no protein was obtained in the pellet fraction as inclusion bodies. The enzyme was purified approx. 10-fold from the crude extracts with a 16 % yield (Table 2). N-terminal amino acid sequencing of the purified recombinant protein resulted in the sequence MKIGVVGLGLIGASL, in complete agreement with the N-terminal sequence deduced from the nucleotide sequence.

MS (matrix-assisted laser-desorption ionization−time-of-flight analysis) resulted in a monomer peak at a molecular mass of 30 210.56, a value almost identical with that predicted from the

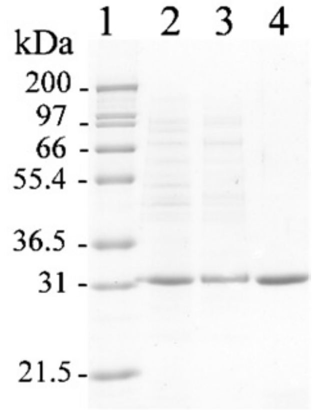

Figure 2 Characterization of the purified recombinant $TyrA_a$

SDS/PAGE (12 % gel) of *Synechocystis* sp. PCC 6803 protein extracts from the *E. coli* transformant harbouring the overexpression construct, pET:*tyrA*$_a$. Lane 1, molecular-mass standards; lane 2, crude extract of transformed cells (6 μg); lane 3, Mono-Q eluate (4 μg); lane 4, affinity-purified protein (4 μg). The purified enzyme displayed a molecular mass of approx. 33 kDa.

Table 2 Purification of recombinant *Synechocystis* $TyrA_a$

Step	Total protein (mg)	Total activity (units)*	Specific activity [nmol · min^{-1} · (μg of protein)$^{-1}$]	Purification factor (fold)
1. Crude extract	280	6.01	21.4	1.0
2. Mono-Q FPLC (P)	160	4.45	27.8	1.3
3. 2′,5′-ADP–Sepharose 4B	4.45	0.98	220	10.3

* mmol/min of TYR produced.

amino acid sequence data. The native molecular mass of $TyrA_a$ was estimated by gel-filtration chromatography as described in the Materials and methods section. A native molecular mass was calculated in the range 57–65 kDa, consistent with the dimeric structure of other TyrA proteins (monomer, 30.2 kDa). Reports in the literature of higher native molecular masses of TyrA proteins from *Corynebacterium* [8] and *Brevibacterium* [8] may indicate that the oligomer species is variable. The higher molecular masses previously reported for *Acinetobacter* [26] and *Ps. aeruginosa* [11] reflect the then unrecognized fusion of *tyrA*$_c$ with another gene of aromatic biosynthesis.

Crude extracts of *E. coli* BL21 (harbouring a plasmid without insert) were used as controls for measuring the extent to which *E. coli* $TyrA_{(p)}$ might contribute to $TyrA_a$ activity. It has been previously reported that AGN is a poor substrate for the *E. coli* $TyrA_{(p)}$ enzyme, which exhibits an absolute requirement for NAD^+ as co-substrate [14]. As expected, none of the $TyrA_a$ activity measured in the presence of $NADP^+$ could be attributed to the $TyrA_{(p)}$ of *E. coli* BL21. The purified recombinant *Synechocystis* $TyrA_a$ showed no activity with prephenate in combination with either $NADP^+$ or NAD^+ as cofactor. $TyrA_a$ activity (AGN/$NADP^+$) was proportional to elapsed time and protein concentration at saturating concentrations of substrates. $TyrA_a$ activity was not detected with AGN in combination with NAD^+.

$TyrA_a$ activity was tested to determine the optimal pH by measuring initial rates of catalysis over a pH range 6.5–10.0 at 25 °C in a variety of buffers as described in the Materials and methods section. No measurements were feasible below a pH of 6.5 due to the acid lability of AGN. The optimum pH of the purified recombinant enzyme was between 8.25 and 8.75. Epps buffer at pH 8.5 was found to be optimal. Lower activities were observed in other buffers at this pH, including Tris/HCl, sodium hydroxide/borate and glycine.

The purified $TyrA_a$ enzyme was less stable during storage at 4 °C than when maintained frozen at −20 °C or at −70 °C. Full activity was retained in repeated freeze–thaw cycles, provided that concentrations of 10 μg of protein/ml or more were maintained. The enzyme displayed an optimum temperature of 28–30 °C, with activity decreasing almost 50 % above 42 °C (results not shown). DTT (up to 0.5 mM) and EDTA/EGTA (up to 5 mM) did not affect enzyme activity. Additionally, no effect on enzymic activity was observed after the addition to standard reaction mixtures of various bivalent metal ions (up to 0.5 mM) including Mg^{2+}, Mn^{2+}, Fe^{2+} or Ca^{2+}.

Confirmation of TYR as the product of $TyrA_a$-mediated catalysis

Figure 3 demonstrates the $NADP^+$-dependent conversion of AGN into TYR. C-18 reverse-phase HPLC was used to analyse reaction mixtures at zero elapsed time (left) and after 30 min of reaction (middle). After the reaction, a fraction of AGN disappeared compared with the zero-time control, and a corresponding amount of TYR product appeared. Unchanged AGN was non-enzymically converted into PHE in the presence of acid ([H^+]), thus confirming the high purity of the AGN substrate preparation. In a comparable experiment using prephenate and $NADP^+$, prephenate was not utilized. When such mixtures were acidified, prephenate was recovered quantitatively as phenylpyruvate. Thus we could conclude that the prephenate had not been scavenged for some unknown reaction and had therefore remained potentially available as a substrate for $TyrA_a$.

Kinetic analysis

Kinetic parameters

Initial-rate measurements taken when varying the concentration of either substrate in the presence of a fixed concentration of the other revealed saturable Michaelis–Menten kinetics. The results were transformed to Lineweaver–Burk double-reciprocal plots (Figures 4A and 4B), useful for displaying results in a form that facilitates derivation of most kinds of equations and that allows visualization of the influence of each substrate on the various slopes or intercepts. Nearly identical V_{max} values were obtained in the series with AGN or $NADP^+$ as variable substrate, confirming the accuracy of the results. The straight lines obtained indicate that the two catalytic sites of the dimer are independent. The converging linear Lineweaver–Burk plots also indicate a ternary-complex (sequential) mechanism. A degree of substrate inhibition was observed at very high concentrations of both AGN and $NADP^+$. A commercial program, GraphPad Prism (version 4.0), from GraphPad Software (San Diego, CA, U.S.A.) was used to estimate kinetic constants directly from non-linear regression by global fitting to the initial velocity equation for a sequential mechanism, and these results are summarized in Table 3. The K_m for $NADP^+$ (38 μM) was almost an order of magnitude smaller than that for AGN (331 μM). The k_{cat}/K_m value, known as the catalytic capture value [27], calculated for AGN was $3.90 \times 10^5\ M^{-1} \cdot s^{-1}$ and the k_{cat}/K_m value for $NADP^+$ was $3.39 \times 10^6\ M^{-1} \cdot s^{-1}$. k_{cat} values were calculated by assuming that the enzyme is a 60.4 kDa homodimer with two active sites.

Plots of Figure 4(A) resulted in lines intersecting at a common point on the abscissa ($1/v_0 = 0$), whereas the intersect in Figure 4(B) is in the second quadrant ($1/v_0 > 0$). The intersect positions indicate the relationship between K_m and the dissociation constant K_{ia} for the variable substrate [28]. Thus the intersect

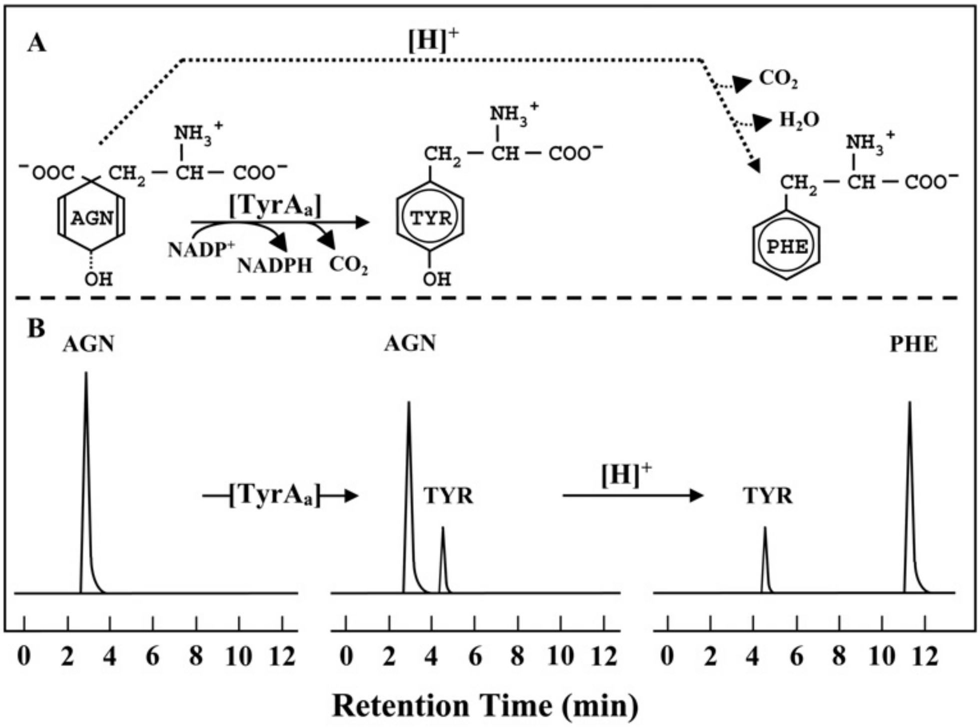

Figure 3 HPLC confirmation of TYR as the product of TyrA$_a$

(**A**) Enzymic reaction catalysed by TyrA$_a$: conversion of AGN and NADP$^+$ to TYR, NADPH and CO_2. The upper dotted-line portion of the schematic illustrates the acid ([H$^+$])-catalysed conversion of AGN to PHE, carbon dioxide and water. (**B**) Reaction samples were analysed by C-18 reverse-phase HPLC as described in the Materials and methods section. At 0 min of elapsed reaction time (left), AGN in the sample eluted at a retention time of approx. 3.5 min. After 30 min of elapsed reaction time (middle), TYR was detected at its retention time of approx. 4.5 min. After acidification of the 30-min reaction mixture (right), AGN was completely converted into PHE, which eluted at a retention time of approx. 11.5 min. Retention times were identical with those obtained for pure standards of AGN, TYR and PHE.

position in Figure 4(A) on the abscissa implies that $K_m = K_{ia}$ for AGN. The intersect position in Figure 4(B), on the other hand, implies that $K_{ia} > K_m$ for NADP$^+$.

Inhibitors

The immediate product of the TyrA$_a$ reaction, TYR, was an effective inhibitor. Double-reciprocal plots (Figures 4C and 4D) showed TYR to be a competitive inhibitor with respect to AGN ($K_i = 89$ μM) and a non-competitive inhibitor ($K_i = 78$ μM) with respect to NADP$^+$. Prephenate, NAD$^+$, NADPH, PHE and 4-hydroxyphenylpyruvate were tested as inhibitors of the *Synechocystis* TyrA$_a$ activity, but none of these produced detectable inhibition. Total insensitivity to NADPH inhibition seems quite striking in view of NADPH inhibition documented for other TyrA homologues, e.g. *E. coli* TyrA$_{(p)}$ [29] and especially TyrA$_a$ from *Arabidopsis* [30].

Although 2′,5′-ADP, as expected, was a competitive inhibitor with respect to NADP$^+$, an unusual relationship with AGN was observed. At high concentrations of AGN, even in combination with low NADP$^+$ concentration, little or no inhibition occurred. When the AGN concentration was lowered to K_m, inhibition up to approx. 40 % could be obtained at the very lowest concentrations of NADP$^+$ technically feasible. Progressively greater inhibition was observed as AGN concentrations were decreased below K_m. Under conditions of sufficiently low AGN concentration, to allow sensitivity to inhibitor, NADP$^+$ could abolish inhibition in a strictly competitive fashion over the tested NADP$^+$ concentration range of 20–75 μM.

A possible explanation for the unexpected effect of AGN on sensitivity to the inhibitor is that 2′,5′-ADP can bind to the E•E$_{agn}$ species (hereafter considered equivalent to the $_{agn}$E•E species), but not to the $_{agn}$E•E$_{agn}$ species. This scenario is depicted in Figure 5, and the scheme shown presumes a high preference for an order of substrate binding whereby AGN binds first. At 331 μM AGN (K_m concentration), the enzyme will partition as follows: 25 % AGN-free dimer (E•E), 25 % $_{agn}$E•E$_{agn}$ dimer and 50 % E•E$_{agn}$ dimer. The proposed sensitive target of inhibitor action (i.e. E•E$_{agn}$) would represent 50 % of the total AGN-bound active sites and therefore 50 % of the total catalytic activity. As the AGN concentration is increased, the relative fraction (F_r) of the enzyme, which is in the $_{agn}$E•E$_{agn}$ form, increases to the F_r^2 value and that of the E•E$_{agn}$ form changes to $\{[AGN]/([AGN] + K_m) - F_r^2\}$. With 0.05 mM AGN the abundance of the E•E$_{AGN}$ species will be more than 14-fold greater than the $_{agn}$E•E$_{agn}$ species. If 2′,5′-ADP selectively targets the E•E$_{agn}$ species, one would expect a correlation between abundance of the E•E$_{agn}$ target and sensitivity of TyrA$_a$ to inhibition by 2′,5′-ADP.

Figure 6 shows the result of fitting the inhibition data to the E•E$_{agn}$-target mechanism proposed. Calculations were performed to relate the expected relative abundance of E•E$_{agn}$ and $_{agn}$E•E$_{agn}$ dimer species that would be generated at a continuum of AGN concentrations (from 0.02 to 1.5 mM). The E•E$_{agn}$ species has one AGN-bound active site, whereas the $_{agn}$E•E$_{agn}$ species has two AGN-bound active sites, and hence each $_{agn}$E•E$_{agn}$ species accounts for twice as much catalytic activity as does each E•E$_{agn}$ species. The upper curve in Figure 6 shows the relative activity that can be attributed to E•E$_{agn}$ (calculated as the number of AGN-bound active sites on E•E$_{agn}$ divided by the total number of AGN-bound active sites present on E•E$_{agn}$ plus $_{agn}$E•E$_{agn}$). When the overall inhibition obtained in the presence of 0.5 mM

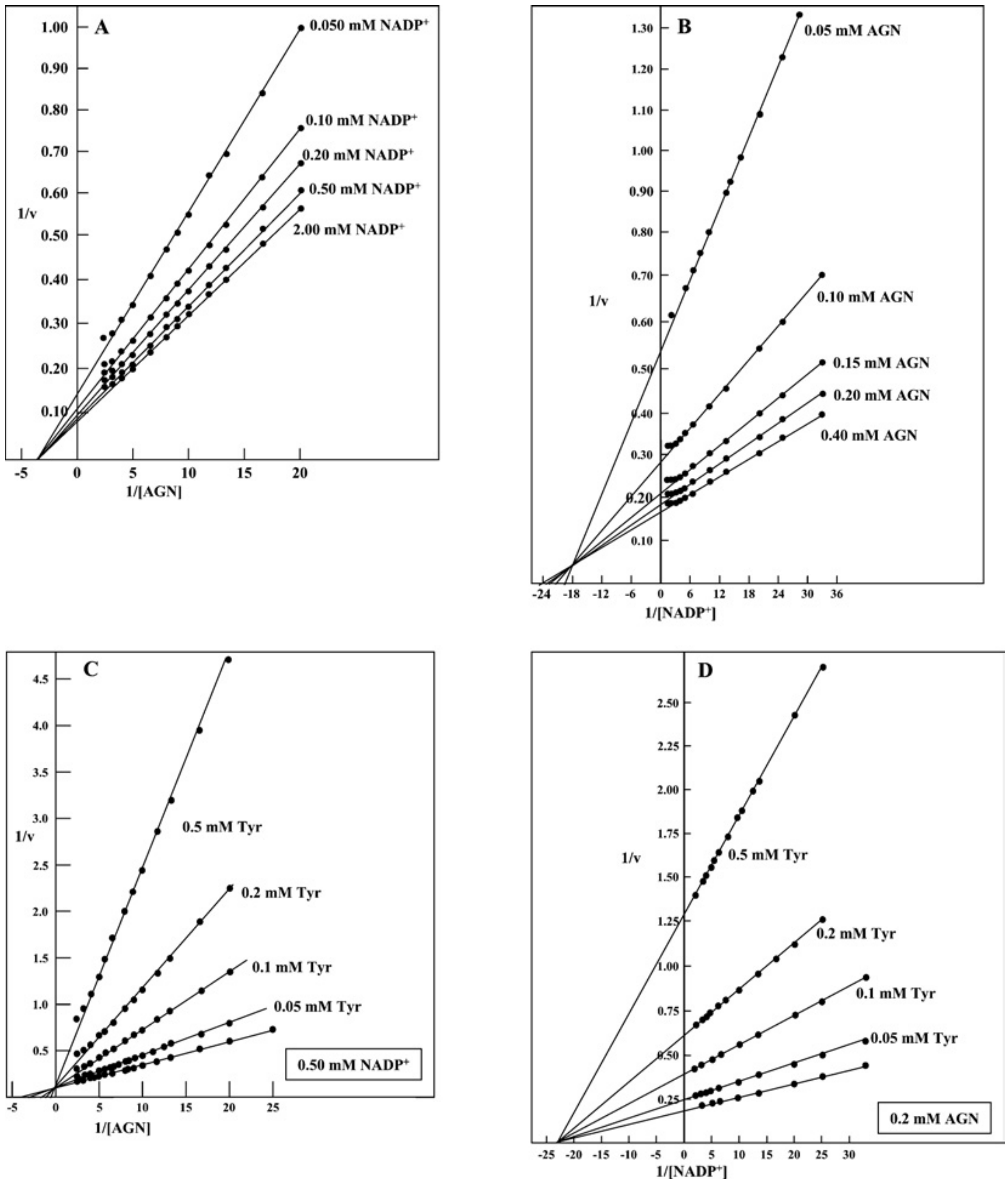

Figure 4 Kinetic analysis of *Synechocystis* TyrA$_a$

Double-reciprocal plots of initial velocities are shown when one substrate was held constant and the other substrate was varied (**A**, **B**) and when TYR was used as inhibitor (**C**, **D**). Slight inhibition was observed at very high concentrations of either substrate. (**A**) $NADP^+$ was held constant at the five concentrations indicated, and AGN concentrations were varied from 0.05 to 0.40 mM. (**B**) AGN was held constant at the five designated concentrations and $NADP^+$ was varied at concentrations from 0.03 to 0.5 mM. (**C**) Varied concentrations of AGN were used with $NADP^+$ concentration fixed at 0.5 mM. Five data sets were obtained in the presence of the four designated TYR concentrations. (**D**) Different concentrations of $NADP^+$ were used with AGN concentration fixed at 0.2 mM. Five data sets were obtained in the presence of the four designated TYR concentrations.

2′,5′-ADP was subtracted from the activity attributed to E•E_{agn} (top line), the resulting data points shown in Figure 6 represent the remaining uninhibited activity attributed to E•E_{agn}. This is very close to a calculated 50 % inhibition of E•E_{agn} that holds throughout the range of AGN concentrations used in Figure 6, as shown by the dotted line.

Thus, even though overall sensitivity to the inhibitor decreased with increasing AGN concentration, the sensitivity of the calculated portion of the total activity contributed by E•E_{agn} was constant (approx. 50 %) under conditions where $NADP^+$ (0.02 mM) and 2′,5′-ADP (0.5 mM) were fixed. Since 0.5 mM 2′,5′-ADP only causes 50 % inhibition of E•E_{agn} at concentrations of $NADP^+$ less than K_m, it seems qualitatively apparent that the K_i value for 2′,5′-ADP must be well over an order of magnitude greater than the K_m value for $NADP^+$ (38 μM).

Kinetics and mechanism of TyrA$_a$

Unlike many dehydrogenases, the reaction catalysed by TyrA$_a$ is irreversible. TYR (having a stable aromatic ring) cannot be converted into AGN (having an unstable cyclohexadienyl ring) in the reverse direction (Figure 1). The reversible binding reactions

Table 3 Kinetic constants of recombinant *Synechocystis* TyrA$_a$

Assays were performed in 50 mM Epps buffer at pH 8.6 and 25 °C. The value calculated for k_{cat} (s^{-1}) was 128.9 ± 9.9.

	K_m (μM)	k_{cat}/K_m ($M^{-1} \cdot s^{-1}$)	K_i (μM)
Substrates tested			
L-Arogenate	331 ± 21.6	3.90×10^5	
Prephenate	N.A.*	N.A.*	†
NADP$^+$	38 ± 1.9	3.39×10^6	
NAD$^+$	N.A.†	N.A.†	†
Inhibitors tested			
L-Tyrosine			89 ± 6.3 (AGN) 78 ± 6.6 (NADP$^+$)

* N.A., no activity when assayed at concentrations up to 3 mM.
† Less than 1 % inhibition was observed using 1.0 mM inhibitor at K_m levels of substrate.

of AGN and NADP$^+$ are followed by the hydride transfer and irreversible decarboxylation, which we assume to be concerted (rather than stepwise) as is the case for the TyrA$_{(p)}$ homologue of *E. coli* [31]. The irreversibility of the reaction dictates that the three rate constants associated with the oxidative decarboxylation, as well as the rate constants k_{off} associated with release of NADPH and TYR, determine the value of k_{cat}.

Since the intercept positions of Figures 4(A) and 4(B) indicate that the K_m and K_{ia} values for AGN are equal but that the K_m value for NADP$^+$ is less than the corresponding dissociation constant, a rapid equilibrium random mechanism can be ruled out since, then, K_a/K_{ia} is expected to equal K_b/K_{ib}. Also, since (as exploited for purification) the enzyme can bind 2′,5′-ADP−Sepharose in the absence of AGN, either a steady-state random mechanism or an ordered mechanism with NADP$^+$ as the first substrate to bind were *a priori* possibilities. However, the fact that TYR inhibits competitively with respect to AGN (Figure 4C) and non-competitively with respect to NADP$^+$ (Figure 4D) eliminated the possibility of an ordered mechanism in which NADP$^+$ is the leading substrate. Although a steady-state random-order mechanism is thus indicated, we favour the possibility that there exists a distinct preference for the binding of AGN first to explain the 2′,5′-ADP inhibition results.

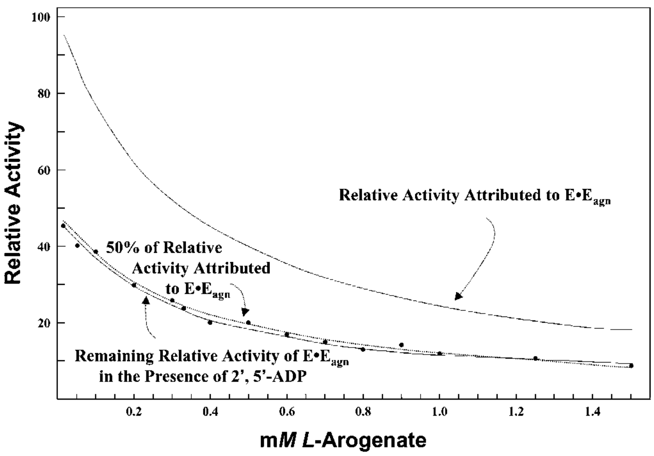

Figure 6 Correlation of fractional enzyme activity contributed by E●E$_{AGN}$ and sensitivity to 2′,5′-ADP

Abundance of enzyme dimers having one catalytic site occupied by AGN (E●E$_{agn}$) or both sites occupied by AGN ($_{agn}$E●E$_{agn}$) was calculated as a function of AGN concentration. The fraction of total catalytic activity that can be attributed to the E●E$_{agn}$ species was determined (top line). Sensitivity to inhibition by 0.5 mM 2′,5′-ADP was determined using 0.02 mM NADP$^+$ and the indicated 15 variable concentrations of AGN. The activity inhibited was subtracted from the calculated relative activities of E●E$_{agn}$ (top line) to yield data points that represent relative activity values of E●E$_{agn}$ remaining in the presence of 2′,5′-ADP.

TyrA$_a$ and prephenate aminotransferase activities in photosynthetic bacteria and algae

TyrA$_a$ specific activities were identified in crude extracts of *P. hollandica*, *P. cruentum* (a red alga), *Chlorella sorokiniana* (a green alga) and in four species of cyanobacteria (Table 4). In these organisms, TyrA$_a$ activity was strictly dependent on NADP$^+$ and no prephenate dehydrogenase activity (NAD$^+$- or NADP$^+$-dependent)

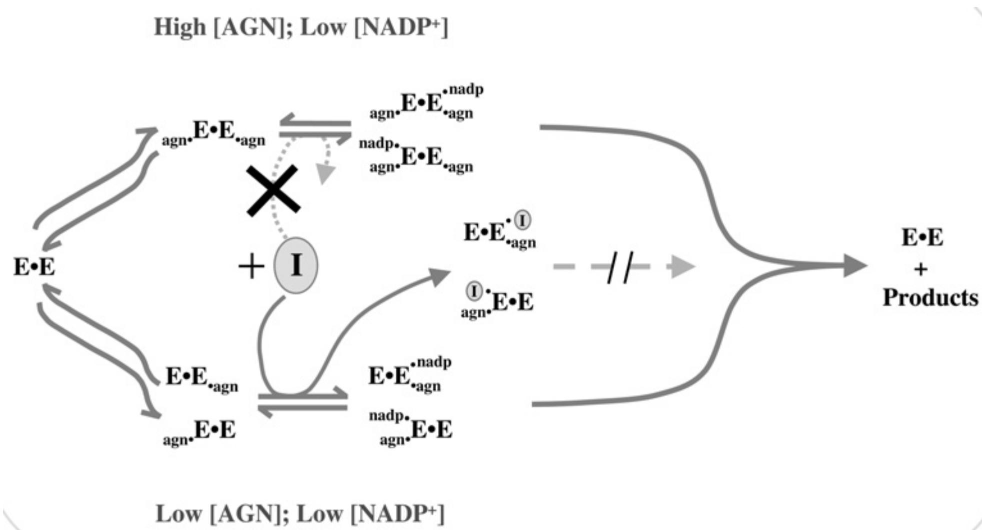

Figure 5 Model for productive catalytic species targeted for inhibition by 2′,5′-ADP

Assuming a strong preference for AGN binding first, the major productive homodimeric complexes present at high AGN concentration (upper pathway) or at low AGN concentration (lower pathway) are shown. If AGN binds first, then high AGN concentrations will eliminate most of the proposed target species (E●E$_{agn}$ or $_{agn}$E●E). The inhibitor (2′,5′-ADP) is shown in grey as an encircled 'I'. A dotted line associated with a 'cross' or with an interruption of continuity indicates inability to bind or lack of activity respectively.

Table 4 Specific activities of $TyrA_a$ and prephenate aminotransferase (PAT) in cyanobacteria, *Chlorophyta*, *Prochlorophyta* and *Rhodophyta*

Organism*	$TyrA_a$ ($nmol \cdot min^{-1} \cdot mg^{-1}$)	PAT ($nmol \cdot min^{-1} \cdot mg^{-1}$)
Synechocystis sp. (ATCC 29108)	14.5	1.91
Anabaena sp. (ATCC 29151)	7.8	0.35
Fisherella sp. (ATCC 29539)	10.9	0.88
Synechococcus sp. (ATCC 27144)†	11.5	0.71
P. hollandica	2.4	0.55
P. cruentum	9.7	1.51
C. sorokiniana	2.4	16.0

* Cyanobacterial and algal species in which only AGN/$NADP^+$ specific activity was determined, i.e. no activity was detected using AGN/NAD^+ or prephenate/NAD(P) combinations.
† Well known in the literature as *Anacystis nidulans* strain Tx 20.

was detected, exactly the features typical of the *Synechocystis* PCC 6803 system. Crude extracts were also assayed for prephenate aminotransferase activity, since the enzyme catalyses the penultimate step in TYR biosynthesis (Figure 1) and yields the substrate for $TyrA_a$. Prephenate aminotransferase activity was found in all the crude extracts tested (Table 4).

Two subtypes of TyrA proteins in heterocystous cyanobacteria

A search of the SWISS-PROT and GenBank® databases identified nine cyanobacterial homologues of *Synechocystis* sp. PCC 6803 *tyrA*$_a$. Two different *tyrA* genes were identified in the genomes of *Anabaena* and in *Nostoc*, and one each from *Synechocystis* (PCC 6803), *Synechococcus* W8102, *Synechococcus* 7002, *Gloeobacter violaceus*, *Prochlorococcus marinus* CCMP1378 and *P. marinus* MED4. When each sequence was used as a query against the BLAST database, it was qualitatively apparent that the ten sequences fell into two subgroups. An alignment of the amino acid sequences of these proteins is shown in Figure 7. The upper subgroup of eight protein sequences (one from each organism) is predicted to comprise $NADP^+$-dependent $TyrA_a$ proteins, since our characterized *S*sp $TyrA_a$ protein falls into this group. These eight proteins cluster tightly on a protein tree (results not shown) in which the position of this TyrA subgroup enjoys strong (100 %) bootstrap support. The bottom two cyanobacterial sequences shown in Figure 7 are quite distinct from the upper ones and belong to a large and cohesive protein subgroup (results not shown) that is dominated by $TyrA_{(p)}$ proteins from the enteric lineage (defined as all organisms that have diverged as far from *E. coli* as *Shewanella putrefaciens* on the 16 S rRNA tree). Residues that are invariant within this latter $TyrA_{(p)}$ subgroup are shown as grey shading in Figure 7. The middle group in Figure 7 consists of experimentally established arogenate-specific dehydrogenases from *Corynebacterium efficiens* (C. A. Bonner and R. A. Jensen, unpublished work), *Corynebacterium glutamicum* [7,8], *Nitrosomonas europaea* [32] and higher plants [15,17,33]. The $TyrA_a$ proteins from coryneform bacteria, *N. europaea*, and higher plants do not cluster closely with one another on the phylogenetic tree (not shown), but we included them in the multiple alignment of Figure 7 in an attempt to visualize a signature motif that might correspond to AGN specificity.

Figure 7 indicates the position of the Wierenga 'fingerprint' [34] for the N-terminal ADP-binding $\beta\alpha\beta$ fold, which is commonly recognized for nicotinamide nucleotide binding. Ssp $TyrA_a$ has the minimal variable loop of two amino acids compared with the maximal five amino acids for the Npu $TyrA_{(p)}$ and Asp $TyrA_{(p)}$ (and *E. coli* $TyrA_{(p)}$). Ssp $TyrA_a$ matches the Wierenga 'fingerprint' residues at positions 1, 2, 4, 6, 8, 11, 15, 18 and 28, but not at positions 30 and 32. It would not be expected to obey the 'fingerprint' at position 32 (D or E), since this negatively charged residue is crucial for hydrogen-bonding to the diol group of the ribose near the adenine moiety in NAD^+-specific enzymes. It is well known that $NADP^+$-specific dehydrogenases cannot tolerate a negatively charged residue at position 32 [35,36]. The general presence of positively charged residues in this region for the $TyrA_a$ proteins, but not for the $TyrA_{(p)}$ or $TyrA_c$ proteins might be significant.

Figure 7 illustrates the anchor residues that are invariant throughout the TyrA superfamily. These residues probably dictate the conserved scaffold responsible for the common chemistry of the separate reactions within the TyrA superfamily. Six additional residues (boxed lightly) are invariant for the currently established $TyrA_a$ proteins (which includes, in addition to cyanobacteria, those from *C. efficiens*, *C. glutamicum*, *N. europaea* and two selected higher-plant sequences). Some of these residues may eventually prove to be tied to narrow specificity for AGN. However, many of them exhibit relatively high conservation throughout the TyrA superfamily, and the apparent invariance quite probably reflects the current small size of the $TyrA_a$ sample. No convincing motif having predictive value for AGN specificity is apparent. One of the conserved arginine residues near the C-termini of the cyanobacterial proteins probably contributes the positively charged side chain that is known [37] to contribute the single most conserved structural feature associated with stabilization of the $NADP^+$−protein complex.

DISCUSSION

Distribution of $TyrA_a$s in nature

Four classes of cyclohexadienyl substrate specificity are known within the TyrA superfamily of homologues. These include prephenate-specific ($TyrA_p$), AGN-specific ($TyrA_a$) and the broad-specificity cyclohexadienyl ($TyrA_c$) dehydrogenases. A fourth class is represented by an enzyme of antibiotic biosynthesis (PapC) that converts 4-amino-4-deoxy-prephenate into 4-aminophenylpyruvate [38]. Representatives of each specificity class have been studied at the molecular-genetic level. Recently, a plant *tyrA*$_a$ has been cloned and characterized from *Arabidopsis thaliana* [33]. Interestingly, the latter consists of two near-identical domains that are fused. The gene encoding this 68 kDa protein co-exists in the genome with a single-domain gene [30] that encodes a predicted 37 kDa protein, somewhat larger than the core catalytic domain of $TyrA_a$ from *Synechocystis*.

The well-studied *E. coli* $TyrA_{(p)}$ differs from *Synechocystis* $TyrA_a$ not only in its substrate specificity, but also in possession of a fused AroQ domain and two allosteric sites, at one of which prephenate acts weakly [39]. The latter differences may not be so surprising, but it is striking how many differences distinguish *Synechocystis* $TyrA_a$ from higher-plant $TyrA_a$ in view of the prevailing hypothesis of endosymbiotic origin. Although both have high specificity for AGN and $NADP^+$, the *Arabidopsis* $TyrA_a$ has a K_m for AGN of 70 μM (compared with 331 μM). It is inhibited by NADPH ($K_i = 54$ μM) and an E–NADPH–AGN dead-end complex has been proposed. One of the two paralogues has a weak ability to utilize prephenate and positive co-operativity for AGN is observed [30].

In photosynthetic eukaryotes, $TyrA_a$ is ubiquitous. In prokaryotes, the $TyrA_a$ class is less widespread and is currently represented by three widely spaced lineages: cyanobacteria, coryneform bacteria and *N. europaea*. This observation is consistent with an evolutionary scenario whereby the ancestral

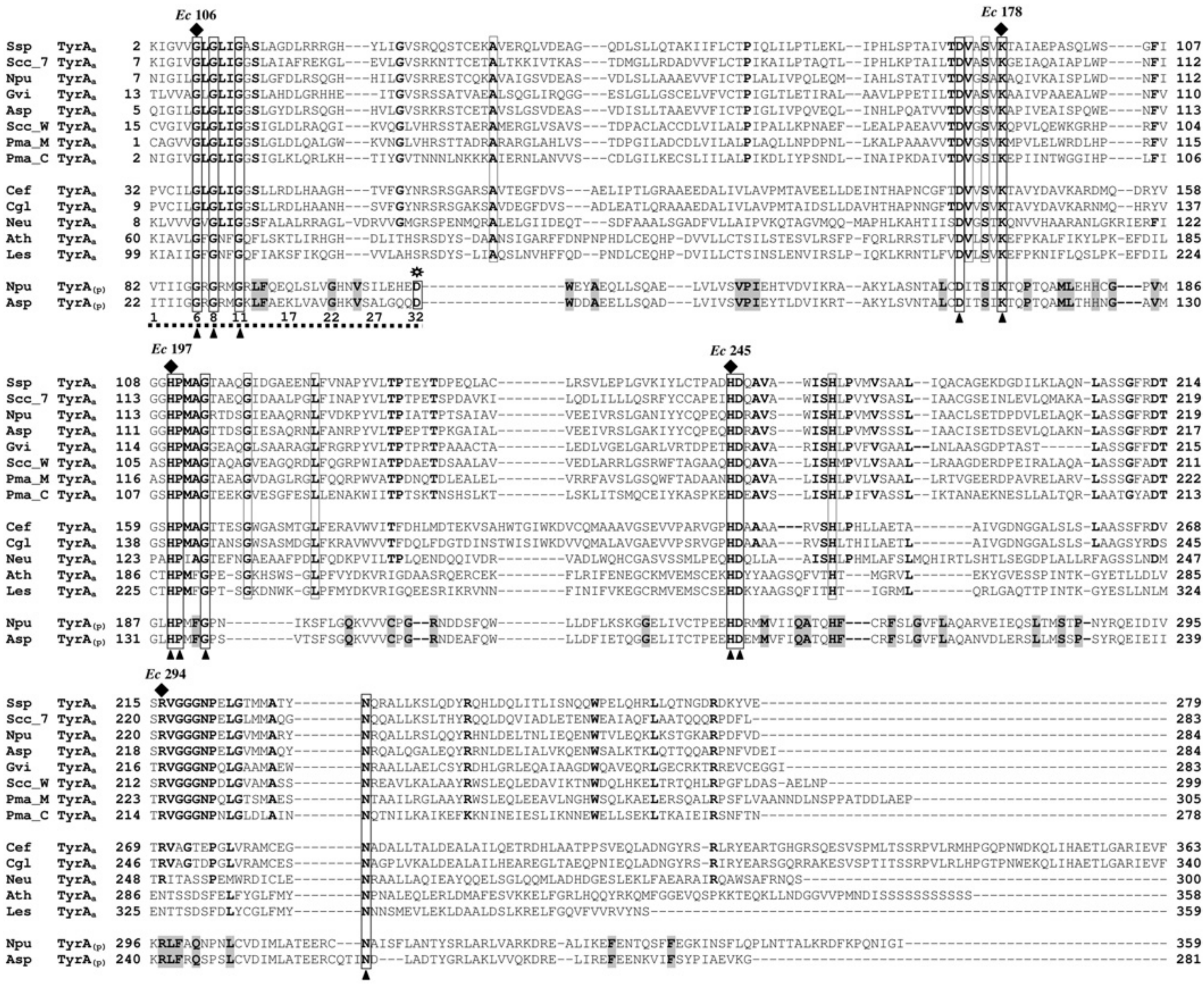

Figure 7 Multiple alignment for comparison of the two subgroups of cyanobacterial TyrA proteins

Organisms: Npu, *Nostoc punctiforme*; Asp, *Anabaena* species; Ssp, *Synechocystis* species; Scc_W and Scc_7, *Synechococcus* species (strains W8102 and 7002); Gvi, *G. violaceus*; Pma_M and Pma_C, *P. marinus* (strains MIT9313 and CCMP1378 MED4); Neu, *N. europaea*; Cef, *C. efficiens*; Cgl, *C. glutamicum*; Ath, *Arabidopsis thaliana*; Les, *Lycopersicon esculentum*. Members of the upper subgroup are $TyrA_a$ proteins (from cyanobacteria). The middle group includes additional known $TyrA_a$ proteins. The lower subgroup, consisting of two cyanobacterial sequences, clusters (results not shown) with the enteric $TyrA_{(p)}$ ('prephenate dehydrogenase') protein subgroup. Anchor residues that are invariant or near-invariant within the entire TyrA protein family are designated with upwardly pointed arrowheads. The aspartate residue of the Wierenga 'fingerprint' [34] that is critical for NAD^+ binding (found only in the lower subgroup) is boxed and designated with an asterisk. The boldface dotted line in the early N-terminal region below the sequences covers the Wierenga 'fingerprint' region, with numbers shown allowing for a maximal variable-loop size of five. Gaps in this region of the alignment are within the variable loop. Conserved residues that are restricted to the $TyrA_a$ grouping of sequences (top and middle blocks) are boxed lightly. The grey-highlighted and boldface residues are those that are invariant or near-invariant within a large set of the enteric $TyrA_{(p)}$ protein subgroup. Residues that are invariant throughout the cyanobacterial $TyrA_a$ grouping, but not shared by all other $TyrA_a$ members, are shown in boldface. Residues marked at the top by black solid diamonds correspond to the amino-acid residue number of the *E. coli* (Ec) $TyrA_{(p)}$ protein.

dehydrogenase was a broad-specificity $TyrA_c$ and in which narrowing of substrate specificity (to yield $TyrA_p$ or $TyrA_a$) has occurred independently on multiple occasions in modern lineages. $TyrA_a$ in higher-plant chloroplasts [17] may have originated from cyanobacteria via endosymbiosis. Assignment of the substrate specificity of experimentally uncharacterized TyrA homologues *in silico* is uncertain unless they exhibit very high amino acid identity with known $TyrA_a$ proteins. For example, the high identities of TyrA sequences from *Mycobacterium tuberculosis*, *Bifidobacterium* (*Thermomonospora*) and *Streptomyces* species with that of *C. glutamicum* suggests a reasonable possibility that actinomycete bacteria as a group will prove to possess the $TyrA_a$ specificity. *N. europaea* currently has no close genome relatives that have been sequenced. The first BLAST hit returned from an *N. europaea* $TyrA_a$ query is the protein from *Ralstonia solanacearum* which is known to differ from that of *N. europaea* in specificity for both of its substrates [32].

The core catalytic domain of TyrA proteins

A core catalytic domain can be identified that is common to all TyrA proteins [19]. Some TyrA proteins have a C-terminal extension that may be an allosteric domain. The simplest set of proteins belonging to the TyrA family exhibit only a core catalytic domain (approx. 180 amino acids). These include the well-characterized $TyrA_c$ enzymes from *Neisseria gonorrhoeae* [32] and *Zymomonas* *mobilis* [40], as well as $TyrA_a$ from the cyanobacteria (the present study). These proteins do not cluster together on the TyrA protein tree. In addition, the core catalytic domain from *Ps. stutzeri* (having a *tyrA*$_c$•*aroF* fusion) has been engineered for study [19]. Xie et al. [19] suggested that the foregoing four TyrA groupings, although divergent from one another, define a common catalytic domain whereby inhibitors bind at the catalytic site and exhibit classical competitive inhibition with respect to the cyclohexadienyl substrates used [19]. In this model, one would expect that the specificity for the side chains of substrates utilized would parallel the specificity for side chains of any inhibitors.

Synechocystis sp. and *A. thaliana* $TyrA_a$ proteins recognize an alanyl side chain in AGN, which in fact is the only cyclohexadienyl substrate that they accept. In line with this, the latter $TyrA_a$ proteins can recognize TYR (alanyl side chain) but not hydroxyphenylpyruvate (pyruvyl side chain) as an inhibitor. The ring-carboxylate moiety of AGN is not essential for binding at the catalytic site since TYR lacks this substituent. On the other hand, since *N. europaea* $TyrA_a$ and *Z. mobilis* $TyrA_c$ are not inhibited by TYR, a 1-carboxy substituent is, probably, necessary for successful binding at the catalytic site. Finally, the *N. gonorrhoeae* $TyrA_{(p)}$ exhibits an overwhelming preference for prephenate (pyruvyl side chain), and, consistent with the above discussion, is subject to inhibition by 4-hydroxyphenylpyruvate (pyruvyl side chain) but not by TYR (alanyl side chain).

The *tyrA*$_c$/*trp* supraoperon of *Nostoc/Anabaena*

All of the cyanobacterial organisms evaluated in the present study possess a highly conserved *tyrA*$_a$ gene, as well as a complete suite of tryptophan-pathway genes that are dispersed (unlinked) in the genome. Curiously, one divergent cyanobacterial lineage of large-genome organisms (*Nostoc* and *Anabaena*) also possesses a *trp/aro* supraoperon consisting of a number of seemingly redundant genes [6,41]. These include a second *tyr*A gene, additional *trp*-pathway genes (all except *trpC*) and genes encoding the first two general steps of aromatic amino acid biosynthesis. All of these linked genes are represented elsewhere in the genomes of *Nostoc* and *Anabaena* at scattered loci. The small-genome cyanobacteria possess single copies of the above genes, all of them at dispersed genomic locations. The closest BLAST hits for the cyanobacterial $TyrA_{(p)}$ proteins are *not* the $TyrA_a$ homologues in these same organisms, but are the $TyrA_{(p)}$ domains of the AroQ•$TyrA_{(p)}$ fusions in the enteric lineage. Since the enteric proteins are NAD^+-specific and strongly prefer prephenate, it is quite possible that the 'extra' cyanobacterial proteins possess a similar specificity pattern. Indeed, this would be consistent with biochemical evidence provided in the literature for both *Nostoc* and *Anabaena* [18].

Specificity for the cyclohexadienyl substrate within the TyrA superfamily

Knowledge of the atomic details of interaction of TyrA proteins with their substrates is limited since X-ray crystallography results are not yet available. Other detailed information is limited to *E. coli*. In retrospect, one can see that *E. coli* $TyrA_{(p)}$ is not the simplest model for studying the basic properties of the catalytic core region because of the *aroQ* fusion. Site-directed mutagenesis has established that H197 (highly conserved amongst all TyrA proteins) of *E. coli* $TyrA_{(p)}$ is an essential catalytic residue [42], and that it specifically interacts with the 4-hydroxy moiety of prephenate. One exception to the invariance of H197 is PapC from *Streptomyces pristinaespiralis*, and this is fully expected since its substrate (4-amino-4-deoxy-prephenate) lacks the 4-hydroxy moiety. In this region, the *E. coli* sequence is ^{197}HPMFG^{201}, compared with NPMFA in *Streptomyces pristinaespiralis* PapC. A second exception is the Sco_2 protein in *Streptomyces coelicolor*, a paralogue of TyrA that resides in the large calcium-dependent antibiotic gene cluster [43]. This predicts that the substrate for Sco_2 TyrA is neither prephenate nor AGN. The alignment match corresponding to the *E. coli* ^{197}HPMFG^{201} motif is APVVG in Sco_2 TyrA. H197 and G201 are otherwise invariant in the TyrA superfamily.

Evidence has also been obtained that R294 interacts electrostatically with the ring carboxylate of prephenate in *E. coli*. Although we suggest (based on sensitivity to TYR inhibition) that $TyrA_a$ from *Synechocystis* sp. PCC 6803, $TyrA_c$ from *Ps. stutzeri* and $TyrA_{(p)}$ from *N. gonorrhoeae* exemplify instances where binding at the catalytic site does not absolutely require a carboxylate ring, R294 is conserved throughout the TyrA superfamily, with the exception of higher plants. Important residues that co-ordinate with the pyruvyl side chain of prephenate (for $TyrA_p$), the alanyl side chain of AGN (for $TyrA_a$) or both (for $TyrA_c$) are unknown, although Christendat and Turnbull [44] have asserted that, in *E. coli*, residues K178, R286 and R294 can at least be eliminated as ones which interact with the pyruvyl side chain of prephenate.

Residues that dictate AGN specificity may be differently influenced by a complex interacting relationship with residues that influence acceptance of NAD^+ and/or $NADP^+$. For example, *C. glutamicum* and *N. europaea* both recognize AGN in a very specific way, but they differ in that the *Corynebacterium* $TyrA_a$ is broadly specific for the pyridine nucleotide cofactor whereas the *Nitrosomonas* $TyrA_a$ is $NADP^+$-specific. Another complexity is that AGN-specific TyrA proteins presumably differ from one another in that the 1-C group must be recognized for AGN-binding in some cases (as for the *Nitrosomonas* $TyrA_a$, since TYR is not an inhibitor), whereas it must not be required for binding in other cases (as for *Synechocystis* $TyrA_a$, since TYR is a potent inhibitor).

Specificity for nicotinamide nucleotide cofactor within the TyrA superfamily

A general axiom of biochemistry holds that dehydrogenases participating in reductive biosynthetic steps utilize NADPH, whereas oxidative catabolic steps utilize NAD^+. Dehydrogenases of oxidative biosynthetic steps (such as the one catalysed by TyrA) belong to neither of the foregoing categories, and some use NAD^+ and others use $NADP^+$ as the redox cofactor. In the vast majority of cases, a strong preference exists within a given protein family for either NAD^+ or $NADP^+$. One exception is the glutamate dehydrogenase family of enzymes, which subdivides into groups exhibiting strict specificity for NAD^+, for $NADP^+$ or those that are broadly specific and can accommodate both [45,46]. There are reports of contemporary TyrA proteins that can use either NAD^+ or $NADP^+$ [47]. Admittedly, results acquired from survey results using crude extracts should be viewed with caution. For example, in crude extracts, $NADP^+$ can readily be converted into NAD^+ by various phosphatases, or prephenate can unexpectedly be a substrate for a separate dehydrogenase, e.g. a broad-specificity lactate dehydrogenase of unknown significance that converts prephenate into prephenyl-lactate [48]. In most cases, where rigorously purified TyrA proteins have been characterized, they have been specific for NAD^+ or for $NADP^+$. *C. glutamicum* $TyrA_a$ does exemplify, however, a well-documented case where either cofactor is accepted, although $NADP^+$ is favoured by almost an order of magnitude [8]. In view of the finding that replacement of T175 by asparagine in NADP-specific aldehyde dehydrogenase of *Vibrio harveyi* resulted in a highly increased utilization of NAD^+ without loss of ability to use $NADP^+$ [49], it is suggestive that the *C. glutamicum TyrA*$_a$ residue homologous with the crucial aspartate of NAD^+-specific TyrA proteins is asparagine. These two dehydrogenases are further similar in that each still possesses a distinct preference for $NADP^+$.

So far, all of the rigorously characterized TyrA$_p$ (from *B. subtilis*) and TyrA$_c$ (from *Z. mobilis*, *Ps. stutzeri* and *Ps. aeruginosa*) proteins are NAD^+-specific. Those cyclohexadienyl dehydrogenases that prefer prephenate over AGN by well over an order of magnitude (denoted TyrA$_{(p)}$) are also NAD^+-specific. These include the TyrA domains of AroQ•TyrA$_{(p)}$ proteins of the enteric lineage, and TyrA$_{(p)}$ from *N. gonorrhoeae*. There is a distinct tendency for prephenate-specific enzymes to prefer NAD^+ and for AGN-specific enzymes to prefer $NADP^+$. Perhaps, there is a structural relationship that favours interaction between the greater positive charge of AGN and the greater negative charge of $NADP^+$ (relative to the prephenate/NAD^+ couple). However, note that in the pseudomonad clade marked by the *tyrA•aroF* fusion, the *Acinetobacter* sp. TyrA is $NADP^+$-specific, whereas the sister subclade *Pseudomonas/Azotobacter* exhibits NAD^+ specificity. Thus the entire clade shares approximately the same profile of cyclohexadienyl substrate preference, even though cofactor specificity has been narrowed in opposite directions.

Physiological ramifications of substrate specificity

A striking feature of oxygenic photosynthetic prokaryotes and eukaryotes is that they have consistently proven to favour the AGN/$NADP^+$ pattern of specificity for TYR biosynthesis, regardless of their fundamental divergence with respect to peripheral antenna proteins and pigments utilized in the photosynthetic process [50,51]. This includes cyanobacteria, *Prochlorophyta*, *Rhodophyta*, unicellular *Chlorophyta* [52] (Table 4), *Euglenophyta* [53] and multicellular *Chlorophyta* [15,23,33]. Since $NADP^+$ is the crucial electron acceptor during photosynthesis and since TYR biosynthesis and maximal growth take place in the light, the favoured utilization of $NADP^+$ may have evolved in response to the mechanisms that enhance the abundance of this cofactor during photosynthesis. Indeed, recent data have been reported to show that the intracellular levels of $NADP^+$ exceed those of NAD^+ by more than an order of magnitude in *Synechocystis* sp. strain PCC 6803 [54]. This is quite striking (a factor difference of approx. 30 or more) in comparison with the 'typical' NAD^+ to $NADP^+$ ratio of approx. 3−5 that is frequently cited in biochemical textbooks [55]. *Pyrococcus furiosus* has recently been shown [56] to possess an $NADP^+$ to NAD^+ ratio that is approx. 4-fold higher than in *E. coli*, and some enzymes that are generally NAD^+-dependent are $NADP^+$-dependent in *P. furiosus*. Thus it appears that the relative pool sizes of these redox cofactors may vary more in nature than previously considered. A potential physiological advantage of the insensitivity of *Synechocystis* TyrA$_a$ to inhibition by NADPH is that even if intracellular levels of NADPH are high as a result of redox flux, TyrA$_a$ is invulnerable to NADPH inhibition. For example, under conditions of high light and low CO_2, the NADPH produced in the photosynthetic light reaction can exceed its utilization with a concomitant relative increase in the reductive state [57]. Insensitivity of TyrA$_a$ to NADPH would allow TYR biosynthesis to be independent of such NADPH flux variations. A mutant lacking type I NADPH dehydrogenase has been isolated in *Synechocystis* sp. PCC 6803, and has been reported [54] essentially to lack oxidized $NADP^+$. This mutant is not auxotrophic for TYR (W. Vermaas, personal communication), presumably because $NADP^+$ gets regenerated very quickly by such processes as CO_2 fixation. Nevertheless, it would be interesting to know whether the mutant might be bradytrophic or hypersensitive to TYR analogue inhibitors.

This is Florida Agriculture Experimental Station Journal series number R-09164.

REFERENCES

1 Todd, A. E., Orengo, C. A. and Thornton, J. M. (2001) Evolution of function in protein superfamilies, from a structural perspective. J. Mol. Biol. **307**, 1113–1143

2 Teichmann, S. A., Rison, S. C. G., Thornton, J. M., Riley, M., Gough, J. and Clothia, C. (2001) The evolution and structural anatomy of the small molecule metabolic pathways in *Escherichia coli*. J. Mol. Biol. **311**, 693–708

3 Stenmark, S. L., Pierson, D. L., Glover, G. I. and Jensen, R. A. (1974) Blue−green bacteria synthesize L-tyrosine by the pretyrosine pathway. Nature (London) **247**, 290–292

4 Patel, N., Pierson, D. L. and Jensen, R. A. (1977) Dual enzymatic routes to L-tyrosine and L-phenylalanine via pretyrosine in *Pseudomonas aeruginosa*. J. Biol. Chem. **252**, 5839–5846

5 Zamir, L. O., Jensen, R. A., Arison, B., Douglas, A., Albers-Schonberg, G. and Bowen, J. R. (1980) Structure of arogenate (pretyrosine), an amino acid intermediate of aromatic biosynthesis. J. Am. Chem. Soc. **102**, 4499–4504

6 Xie, G., Keyhani, N. O., Bonner, C. A. and Jensen, R. A. (2003) The ancient origin of the tryptophan operon and tracking the subsequent dynamics of evolutionary change. Microbiol. Mol. Biol. Rev. **67**, 303–342

7 Fazel, A. M., Bowen, J. R. and Jensen, R. A. (1980) Arogenate (pretyrosine) is an obligatory intermediate of L-tyrosine biosynthesis: confirmation in a microbial mutant. Proc. Natl. Acad. Sci. U.S.A. **77**, 1270–1273

8 Fazel, A. M. and Jensen, R. A. (1979) Obligatory biosynthesis of L-tyrosine via the pretyrosine branchlet in coryneform bacteria. J. Bacteriol. **138**, 805–815

9 Fazel, A. M. and Jensen, R. A. (1980) Regulation of prephenate dehydratase in coryneform species of bacteria by L-phenylalanine and by remote effectors. Arch. Biochem. Biophys. **200**, 165–176

10 Whitaker, R. J., Byng, G. S., Gherna, R. L. and Jensen, R. A. (1981) Diverse enzymological patterns of phenylalanine biosynthesis in pseudomonads are conserved in parallel with deoxyribonucleic acid homology groupings. J. Bacteriol. **147**, 526–534

11 Xia, T. and Jensen, R. A. (1990) A single cyclohexadienyl dehydrogenase specifies the prephenate dehydrogenase and arogenate dehydrogenase components of the dual pathways to L-tyrosine in *Pseudomonas aeruginosa*. J. Biol. Chem. **265**, 20033–20036

12 Calhoun, D. H., Bonner, C. A., Gu, W., Xie, G. and Jensen, R. A. (2001) The emerging periplasm-localized subclass of AroQ chorismate mutases, exemplified by those from *Salmonella typhimurium* and *Pseudomonas aeruginosa*. Genome Biol. **2**, 0030.1–0030.16

13 Zhao, G., Xia, T., Fischer, R. S. and Jensen, R. A. (1992) Cyclohexadienyl dehydratase from *Pseudomonas aeruginosa*: molecular cloning of the gene and characterization of the gene product. J. Biol. Chem. **267**, 2487–2493

14 Ahmad, S. and Jensen, R. A. (1987) The prephenate dehydrogenase component of the bifunctional T-protein in enteric bacteria can utilize L-arogenate. FEBS Lett. **216**, 133–139

15 Gaines, C. G., Byng, G. S., Whitaker, R. J. and Jensen, R. A. (1982) L-tyrosine regulation and biosynthesis via arogenate dehydrogenase in suspension-cultured cells of *Nicotiana silvestris* (Speg. et Comes). Planta **156**, 233–240

16 Connelly, J. A. and Conn, E. E. (1986) Tyrosine biosynthesis in *Sorghum bicolor*: isolation and regulatory properties of arogenate dehydrogenase. Z. Naturforsch **41c**, 69–78

17 Jensen, R. A. (1986) Tyrosine and phenylalanine biosynthesis: relationship between alternative pathways, regulation and subcellular location. Recent Adv. Phytochem. **20**, 57–82

18 Hall, G. C., Flick, M. B., Gherna, R. L. and Jensen, R. A. (1982) Biochemical diversity for biosynthesis of aromatic amino acids among the cyanobacteria. J. Bacteriol. **149**, 65–78

19 Xie, G., Bonner, C. A. and Jensen, R. A. (2000) Cyclohexadienyl dehydrogenase from *Pseudomonas stutzeri* exemplifies a widespread type of tyrosine-pathway dehydrogenase in the TyrA protein family. Comp. Biochem. Physiol. C **125**, 65–83

20 Bonner, C. A., Fischer, R. S., Ahmad, S. and Jensen, R. A. (1990) Remnants of an ancient pathway to L-phenylalanine and L-tyrosine in enteric bacteria: evolutionary implications and biotechnological impact. Appl. Environ. Microbiol. **56**, 3741–3747

21 Kaneko, T., Sato, S., Kotani, H., Tanaka, A., Asamizu, E., Nakamura, Y., Miyajima, N., Hirosawa, M., Sugiura, M., Sasamoto, S. et al. (1996) Sequence analysis of the genome of the unicellular cyanobacterium *Synechocystis* sp. strain PCC6803. II. Sequence determination of the entire genome and assignment of potential protein-coding regions. DNA Res. **3**, 109–136

22 Bonner, C. A. and Jensen, R. A. (1987) Arogenate dehydrogenase. Methods Enzymol. **142**, 488–494

23 Bonner, C. A. and Jensen, R. A. (1987) Prephenate aminotransferase. Methods Enzymol. **142**, 479–487

24 Bradford, M. M. (1976) A rapid and sensitive method for the quantitation of microgram quantities of protein utilizing the principle of protein−dye binding. Anal. Biochem. **72**, 680–685
25 Laemmli, U. K. (1970) Cleavage of structural proteins during the assembly of the head of bacteriophage T4. Nature (London) **227**, 680–685
26 Byng, G. S., Berry, A. and Jensen, R. A. (1985) Evolutionary implications of features of aromatic amino acid biosynthesis in the genus *Acinetobacter*. Arch. Microbiol. **143**, 122–129
27 Northrup, D. B. (1999) Rethinking fundamentals of enzyme action. Adv. Enzymol. Rel. Areas Mol. Biol. **73**, 15–55
28 Rudolph, F. B. and Fromn, H. J. (1979) Plotting methods for analyzing enzyme rate data. Methods Enzymol. **63**, 138–159
29 Sampathkumar, P. and Morrison, J. F. (1982) Chorismate mutase-prephenate dehydrogenase from *Escherichia coli*. Kinetic mechanism of the prephenate dehydrogenase reaction. Biochim. Biophys. Acta **702**, 212–219
30 Rippert, P. and Matringe, M. (2002) Purification and kinetic analysis of the two recombinant arogenate dehydrogenase isoforms of *Arabidopsis thaliana*. Eur. J. Biochem. **269**, 4753–4761
31 Hermes, J. D., Tipton, P. A., Fisher, M. A., O'Leary, M. H., Morrison, J. F. and Cleland, W. W. (1984) Mechanisms of enzymatic and acid-catalyzed decarboxylations of prephenate. Biochemistry **23**, 6263–6275
32 Subramaniam, P., Bhatnagar, R., Hooper, A. and Jensen, R. A. (1994) The dynamic progression of evolved character states for aromatic amino acid biosynthesis in Gram-negative bacteria. Microbiology **140**, 3431–3440
33 Rippert, P. and Matringe, M. (2002) Molecular and biochemical characterization of an *Arabidopsis thaliana* arogenate dehydrogenase with two highly similar and active protein domains. Plant Mol. Biol. **48**, 361–368
34 Wierenga, R. K., Terpstra, P. and Hol, W. G. J. (1986) Prediction of the occurrence of the ADP-binding $\beta\alpha\beta$-fold in proteins, using an amino-acid sequence fingerprint. J. Mol. Biol. **187**, 101–107
35 Fan, F., Lorenzen, J. A. and Plapp, B. V. (1991) An aspartate residue in yeast alcohol dehydrogenase I determines the specificity for coenzyme. Biochemistry **30**, 6397–6401
36 Feeney, R., Clarke, A. R. and Holbrook, J. J. (1990) A single amino acid substitution in lactate dehydrogenase improves the catalytic efficiency with an alternative coenzyme. Biochem. Biophys. Res. Commun. **166**, 667–672
37 Carugo, O. and Argos, P. (1997) NADP-dependent enzymes. I: conserved stereochemistry of cofactor binding. Proteins: Struct. Funct. Genet. **28**, 10–28
38 Blanc, V., Gil, P., Bamasjacques, N., Lorenzon, S., Zagorec, M. and Schleuniger, J. (1997) Identification and analysis of genes from *Streptomyces pristinaespiralis* encoding enzymes involved in the biosynthesis of the 4-dimethylamino-L-phenylalanine precursor of pristinamycin I. Mol. Microbiol. **23**, 191–202
39 Turnbull, J. L., Morrison, J. F. and Cleland, W. W. (1991) Kinetic studies on chorismate mutase-prephenate dehydrogenase from *Escherichia coli*: models for the feedback inhibition of prephenate dehydrogenase by L-tyrosine. Biochemistry **30**, 7783–7788
40 Zhao, G., Xia, T., Ingram, L. and Jensen, R. A. (1993) An allosterically insensitive class of cyclohexadienyl dehydrogenase from *Zymomonas mobilis*. Eur. J. Biochem. **212**, 157–165
41 Xie, G., Bonner, C. A., Brettin, T. T., Gottardo, R., Keyhani, N. and Jensen, R. A. (2003) Lateral gene transfer and ancient paralogy of operons containing redundant copies of tryptophan-pathway genes in *Xylella* species and heterocystous cyanobacteria. Genome Biol. **4**, R14
42 Christendat, D., Saridakis, V. C. and Turnbull, J. L. (1998) Use of site-directed mutagenesis to identify residues specific for each reaction catalyzed by chorismate mutase-prephenate dehydrogenase from *Escherichia coli*. Biochemistry **37**, 15703–15712
43 Ryding, N. J., Anderson, T. B. and Champness, W. C. (2002) Regulation of the *Streptomyces coelicolor* calcium-dependent antibiotic by *absA*, encoding a cluster-linked two-component system. J. Bacteriol. **184**, 794–805
44 Christendat, D. and Turnbull, J. L. (1999) Identifying groups involved in the binding of prephenate to prephenate dehydrogenase from *Escherichia coli*. Biochemistry **38**, 4782–4793
45 Baker, P. J., Britton, K. L., Engel, P. C., Farrants, G. W., Lilley, K. S., Rice, D. W. and Stillman, T. S. (1999) Subunit assembly and active site location in the structure of glutamate dehydrogenase. Proteins **12**, 75–86
46 Miñambres, B., Olivera, E. R., Jensen, R. A. and Luengo, J. M. (2000) A new class of glutamate dehydrogenases (GDH). Biochemical and genetic characterization of the first member, the AMP-requiring NAD-specific GDH of *Streptomyces clavuligerus*. J. Biol. Chem. **275**, 39529–39542
47 Byng, G. S., Whitaker, R. J., Gherna, R. L. and Jensen, R. A. (1980) Variable enzymological patterning in tyrosine biosynthesis as a means of determining natural relatedness among the *Pseudomonadaceae*. J. Bacteriol. **144**, 247–257
48 Zamir, L. O., Tiberio, R., Devor, K. A., Sauriol, F., Ahmad, S. and Jensen, R. A. (1988) Structure of D-prephenyllactate. A carboxycyclohexadienyl metabolite from *Neurospora crassa*. J. Biol. Chem. **263**, 17284–17290
49 Zhang, L., Ahvazi, B., Szittner, R., Vrielink, A. and Meighen, E. (1999) Change of nucleotide specificity and enhancement of catalytic efficiency in single point mutants of *Vibrio harveyi* aldehyde dehydrogenase. Biochemistry **38**, 11440–11447
50 Tomitani, A., Okada, K., Miyashita, H., Matthijs, H. C. P., Ohno, T. and Tanaka, A. (1999) Chlorophyll b and phycobilins in the common ancestor of cyanobacteria and chloroplasts. Nature (London) **400**, 159–162
51 Grabowski, B., Cunningham, J. F. X. and Gantt, E. (2001) Chlorophyll and carotenoid binding in a simple red algal light-harvesting complex crosses phylogenetic lines. Proc. Natl. Acad. Sci. U.S.A. **98**, 2911–2916
52 Bonner, C. A., Fischer, R. S., Schmidt, R. R., Miller, P. W. and Jensen, R. A. (1995) Distinctive enzymes of aromatic amino acid biosynthesis that are highly conserved in land plants are also present in the chlorophyte alga *Chlorella sorokiniana*. Plant Cell Physiol. **36**, 1013–1022
53 Byng, G. S., Whitaker, R. J., Shapiro, C. L. and Jensen, R. A. (1981) The aromatic amino acid pathway branches at L-arogenate in *Euglena gracilis*. Mol. Cell. Biol. **1**, 426–438
54 Cooley, J. W. and Vermaas, W. F. J. (2001) Succinate dehydrogenase and other respiratory pathways in thylakoid membranes of *Synechocystis* sp. strain PCC 6803: capacity comparisons and physiological function. J. Bacteriol. **183**, 4251–4258
55 Kaplan, N. O. (1960) The pyridine coenzymes. In The Enzymes, 2nd edn, vol. 3 (Boyer, P. D., Lardy, H. and Myrback, K., eds.), pp. 105–169, Academic Press, New York
56 Pan, G., Verhagen, M. F. J. M. and Adams, M. W. W. (2001) Characterization of pyridine nucleotide coenzymes in the hyperthermophilic archaeon *Pyrococcus furiosus*. Extremophiles **5**, 393–398
57 Heber, U., Bligny, R., Streb, P. and Douce, R. (1996) Photorespiration is essential for the protection of the photosynthetic apparatus of C3 plants against photoinactivation under sunlight. Bot. Acta **109**, 307–315
58 Jensen, R. A. and Gu, W. (1996) Evolutionary recruitment of biochemically specialized subdivisions of family I within the protein superfamily of aminotransferases. J. Bacteriol. **178**, 2161–2171

Received 25 November 2003/11 May 2004; accepted 1 June 2004
Published as BJ Immediate Publication 1 June 2004, DOI 10.1042/BJ20031809